JOURNAL OF GEOPHYSICAL RESEARCH, VOL. 91, NO. A1, PAGES 143–153, JANUARY 1, 1986

Beat Excitation of Whistler Mode Sidebands Using the Siple VLF Transmitter

R. A. HELLIWELL, U. S. INAN, J. P. KATSUFRAKIS, AND D. L. CARPENTER

Space, Telecommunications, and Radioscience Laboratory, Stanford University, California

The process of whistler mode sideband generation in the magnetosphere was studied by transmitting two monochromatic signals closely spaced in frequency (Δf = 5–45 Hz) from the experimental VLF transmitter at Siple Station, Antarctica. The signals were observed following ducted magnetospheric propagation to the conjugate station at Roberval, Quebec. Sidebands up to seventh order were generated extending to ±100 Hz with respect to the average frequency of the carriers. New frequencies were observed both under conditions of little or no growth of the input signals and when one of the input signals did grow significantly. At times the sideband amplitudes exceeded the intensity of either input signal. A small signal mechanism is proposed in which emissions are triggered by each beat between the input waves but are then suppressed by the following beat. The energy from the phase bunched particles is believed to feed preferentially into the sidebands rather than causing growth of the input waves themselves. In this model, phase trapping of resonant electrons by the wave is not required. The observed process of sideband generation provides a mechanism to break down the coherence of relatively narrowband waves in the magnetosphere and may thus account for existing evidence of the transformation of relatively coherent wave packets into broader more variable bands of noiselike signals.

1. INTRODUCTION

The earth's magnetosphere is known to amplify VLF whistler mode electromagnetic waves by as much as 1000-fold in power [*Helliwell and Katsufrakis*, 1978]. Whistler mode waves cause precipitation of energetic electrons into the ionosphere where they produce X rays, light emissions, and enhanced ionization [*Rosenberg et al.*, 1971; *Helliwell et al.*, 1980; *Inan et al.*, 1982]. Whistler mode waves originate in atmospheric lightning, VLF transmitters, power grids, and spontaneous emission within the magnetosphere. Their spectral properties are used for diagnostics of both the thermal plasma [*Park and Carpenter*, 1978] and the energetic electrons that are trapped in the radiation belts [*Carlson et al.*, 1985].

Although much is known about whistler mode waves and the effects they cause, the basic mechanism of their growth is still not understood. However, there is widespread agreement that the mechanism is based on Doppler shifted cyclotron resonance between the waves and counter streaming energetic (1–100 keV) electrons (see *Matsumoto* [1979] for a review of theories). An outstanding and puzzling feature of many whistler mode signals is their small bandwidth. Narrowband whistler mode signals are preferentially amplified compared with broadband signals. Emissions triggered by narrowband signals are usually also narrow in bandwidth, but their center frequencies vary slowly with time. The term coherent wave instability (CWI) has been used to describe the generation process of narrowband VLF emissions, and a simple feedback mechanism has been suggested to explain it [*Helliwell and Inan*, 1982].

Following the unexpected experimental observation of sidebands [*Helliwell*, 1983], a new experiment on sideband generation has been carried out with the VLF transmitter at Siple Station, Antarctica. Sidebands are important for two reasons. First, they constitute an important clue as to the mechanism of VLF emission generation. Second, they serve to broaden the spectrum of VLF signals in a plasma, thus altering the conditions for growth and triggering [*Raghuram et al.*, 1977]. Sidebands were generated by simultaneously injecting into the magnetosphere two monochromatic signals closely spaced in frequency. In experiments of this type the signals are assumed to travel in a magnetospheric duct to the conjugate point located at Roberval, Quebec, as shown in Figure 1. Near the equatorial plane the ducted signals first undergo temporal growth and then they trigger emissions [*Helliwell and Katsufrakis*, 1974]. When only one frequency is transmitted, the wave usually grows 20–40 dB and triggers rising emissions. However, when two or more frequencies are transmitted with spacings less than about 100 Hz, growth is reduced and the character of triggering changes. Growth may be suppressed at one or both of the injected frequencies [*Helliwell*, 1983], and sidebands may be generated. In this paper an experiment is described in which the observed sidebands are associated with discrete emissions that appear to be triggered by each of the beats between the input waves. From these results a new model of sideband generation is inferred that does not necessarily depend on the trapping of resonant electrons in the potential well of the wave.

2. DESCRIPTION OF EXPERIMENT

Two coherent signals of variable relative amplitude and frequency spacing are transmitted in a variety of patterns. Examples of the spectrum before and after transmission through the magnetosphere are shown in Figures 2*a* and 2*b*, respectively. The two carriers, f_1 and f_2, have equal amplitude and are spaced 20 Hz apart. Two days, June 30 and July 11, 1983, are represented; in Figure 2*a*, f_1 and f_2 are 2300 and 2320 Hz, while in Figure 2*b*, they are 3750 and 3770 Hz. As received at Palmer Station, 1400 km to the north of Siple Station, the spectrum (Figure 2*a*) shows weak (~25 dB down) first-order sidebands that are attributed to nonlinear-

Paper number 5A8768.
0148-0227/86/005A-8768$05.00

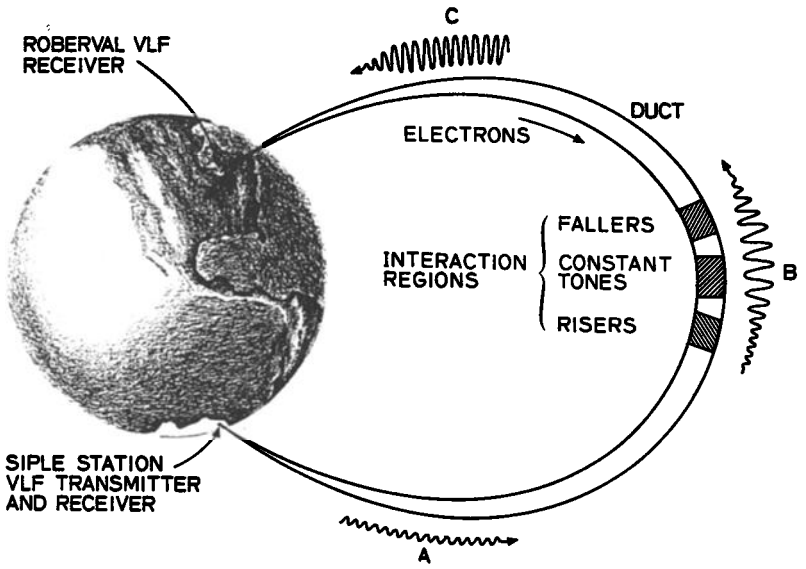

Fig. 1. Sketch of ducted VLF propagation between Siple Station, Antarctica, and Roberval, Quebec. Waves are temporally amplified through doppler-shifted cyclotron resonance with counterstreaming electrons in interaction regions near the equatorial plane, a process that commonly leads to the triggering of emissions.

ity in the class AB broadband power (~150 kW) amplifier of the Siple transmitter. After transmission through a magnetospheric duct to Roberval, the spectrum (Figure 2*b*) shows strong first-order sidebands as well as weaker sidebands up to third-order.

Examples of the dynamic spectrum at Roberval are shown in Figures 3*a* and 3*b*. In Figures 3*a* and 3*b* the top, middle, and bottom panels show total amplitude in decibels, dynamic spectrum of the received signal, and the transmitted format (aligned with the strongest components of the received signal). In Figure 3*a* a 2-s pulse is overlapped with a 1-s pulse of the same amplitude but 20 Hz lower in frequency. We see exponential growth to saturation followed by the triggering of emissions. (Vertical lines on the spectra are sferics generated by atmospheric lightning.) When the second signal is turned on at $t = 4$ s the intensity of the first

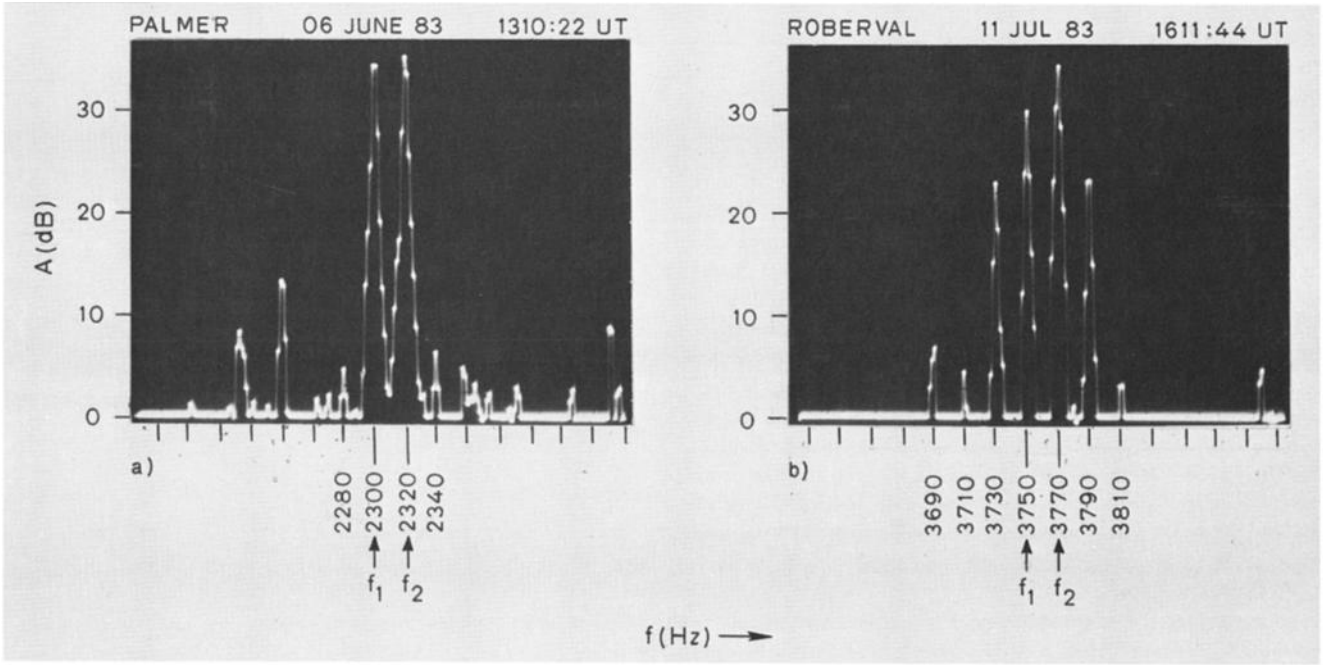

Fig. 2. (*a*) A sample of transmitted spectrum as received on June 6, 1983, 1310:22 UT, at Palmer, Antarctica, showing two carriers at 2300 Hz and 2320 Hz, and two first-order sidebands believed to be generated in the transmitter at ~30 dB relative to the carriers. Other responses shown on the spectrum are attributed to extraneous noise. (*b*) Sample of whistler mode signals as received at Roberval on July 11, 1983, 1611:44 UT, showing the two carriers at 3750 Hz and 3770 Hz together with first-, second-, third-, and fourth-order sidebands, believed to be generated in the magnetosphere. In both spectra the filter bandwidth was 1.6 Hz.

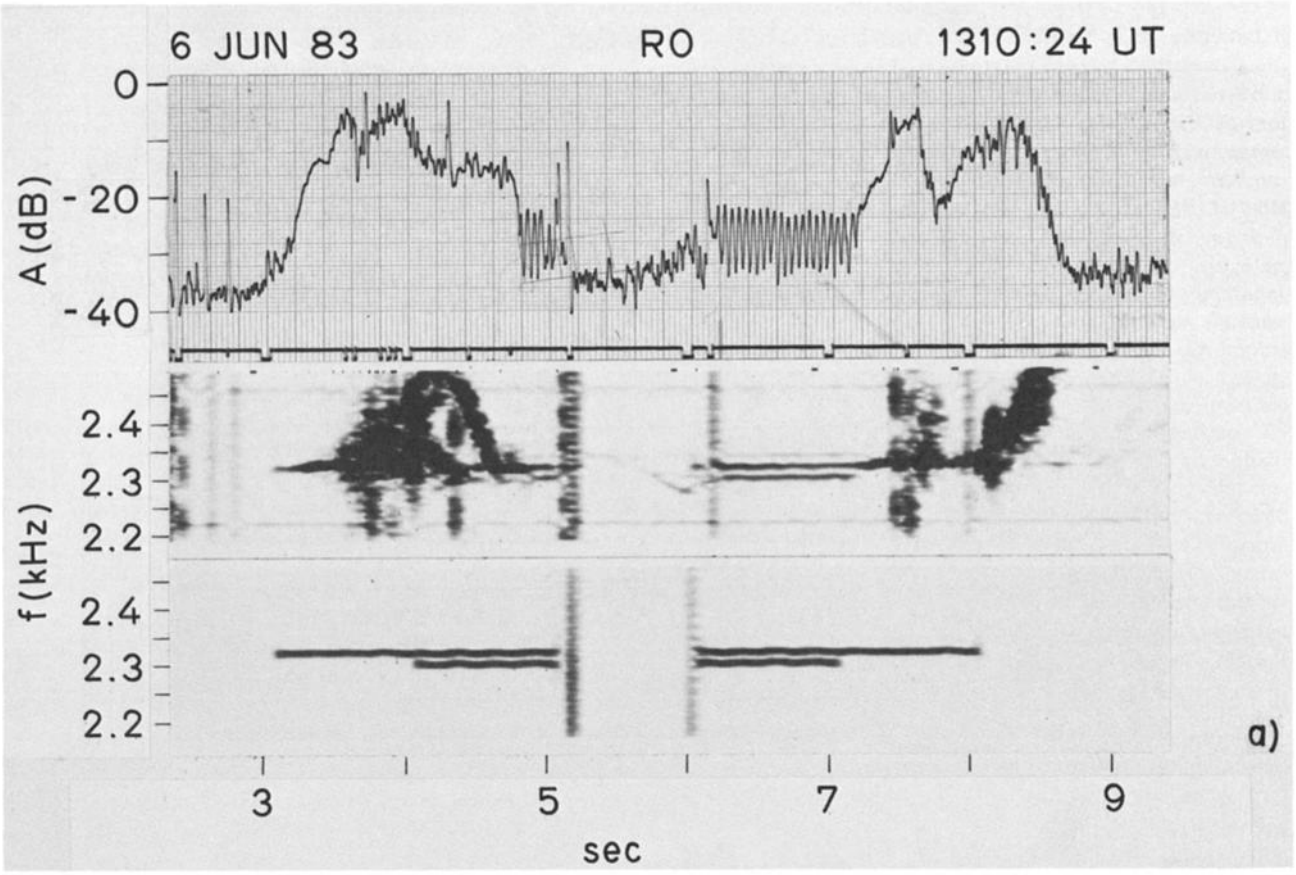

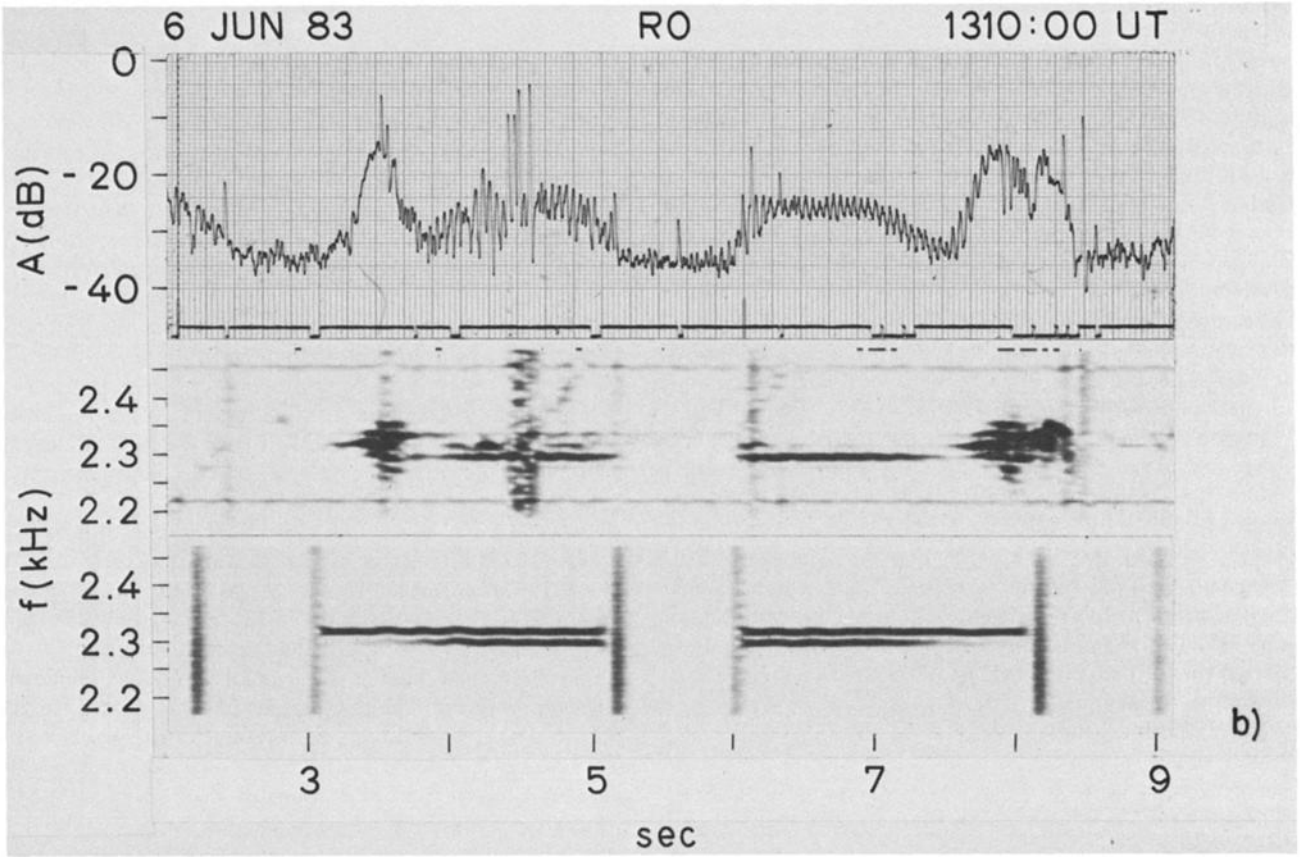

Fig. 3. Two-frequency response at Roberval for June 6, 1983 are shown. Total amplitude in decibels; dynamic spectrum of the received signal and the transmitted format are shown in the top, middle, and bottom panels, respectively. (*a*) $\Delta f = 20$ Hz, lower carrier f_1 off in 3–4 s and 7–8 s intervals. (*b*) $\Delta f = 20$ Hz, f_1 increased in intensity at 20 dB/s in 3–4 s interval and decreased at 20 dB/s in the 7–8 s interval.

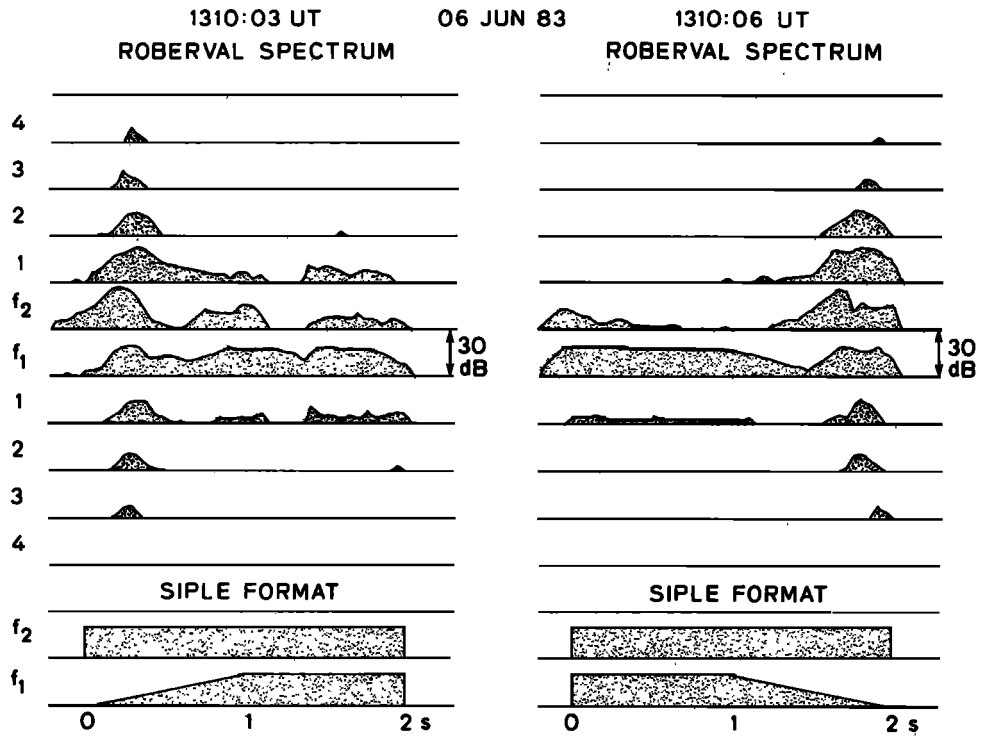

Fig. 4. Amplitude versus time for all components of the spectrum in Figure 3*b*. Each line shows the amplitude of a particular frequency component on a relative scale of 30 dB. f_1 and f_2 are the transmitted carriers, while the single digits refer to the order of the upper (top) and lower (bottom) sideband frequencies.

carrier drops rapidly to the unamplified level, as evidenced by the beat pattern that appears when the emissions are no longer present (after 4.8 s) in the filter passband. When the experiment is repeated 1 s later (at $t = 6$ s) in reverse order, with the two carriers being switched on together, this beat pattern reappears with no evidence of temporal growth. After 1 s the lower signal is turned off. The upper signal then immediately begins to grow at the same exponential rate observed during the first single pulse, as shown in the top panel. In this experiment it is clear that recovery from suppression is essentially instantaneous, in contrast to the so-called quiet band effect [*Raghuram et al.*, 1977; *Cornilleau-Wehrlin and Gendrin*, 1979], in which background noise was suppressed in a narrow band below the carrier, with a delay in onset and recovery of about 10 s.

Figure 3*b* shows a similar experiment except that during the intervals $t = 3$–4 s and $t = 7$–8 s, the signal intensity at the lower frequency is gradually changed (either up or down) at the rate of 20 dB/s. Strong sidebands are observed when the intensity of the lower frequency signal is ~12–15 dB lower than that of the upper signal. This enhanced sideband activity is tentatively attributed to the combination of relatively strong growth of the stronger input signal and modulation of this amplified signal by the beat between the two input signals.

The intensities of the carriers and the sidebands of the spectra of Figure 3*b* are shown in Figure 4. The carriers are designated f_1 and f_2, while integers indicate separations of multiples of $\Delta f = 20$ Hz from the nearest carrier. Sidebands up to fourth order are seen. The signal ratio at which the sideband order is a maximum is somewhat uncertain because of propagation on multiple magnetospheric paths, a corresponding spread in group delays, and hence an extension of the length of the received signal by ~200 ms. The format is aligned with respect to the delay of the strongest echo, which in this case shows the greatest delay. It is interesting to note in Figure 4 that the signal at f_1, as it is ramping down, begins to grow at the same time the sidebands develop. It appears that the growth at f_1 may in fact be a sideband resulting from the interaction between f_2 and the first order upper sideband at $f_2 + \Delta f$. Consistent with this suggestion is the fact that the sideband structure near the end of the down ramp is symmetrical about f_2 rather than the average frequency $(f_1 + f_2)/2$ of the two input signals. In Figure 3*b* the relatively low amplitude of the f_2 carrier is attributed to multipath fading, as in Figure 5, discussed below.

Sidebands appear over a wide range of Δf, as illustrated in Figure 5 from the period of Figure 3. In this case the signal separation frequency is increased continuously from 5 to 45 Hz over a 5-s interval, while keeping f_1 constant. Between $\Delta f = 5$ Hz and $\Delta f = 16$ Hz temporal growth of order ~10 dB is observed, although a sharp drop of 5–10 dB is seen between beat peaks. Sidebands up to sixth or seventh order can be detected. For $\Delta f > 16$ Hz the amplitude drops to approximately the unamplified level. In this range of Δf a relatively clear beat is seen and the sideband intensity has been reduced. The fluctuations in average amplitude of the total field (top panel) are attributed to the change in frequency of the upper component which alters the relative phase of multiple path components.

The mechanism of sideband generation is suggested by other examples, shown in Figure 6, from a period when sideband levels were relatively higher. In these cases the transmitted format is shown above. To help resolve time and frequency effects, the spectra are then shown for three

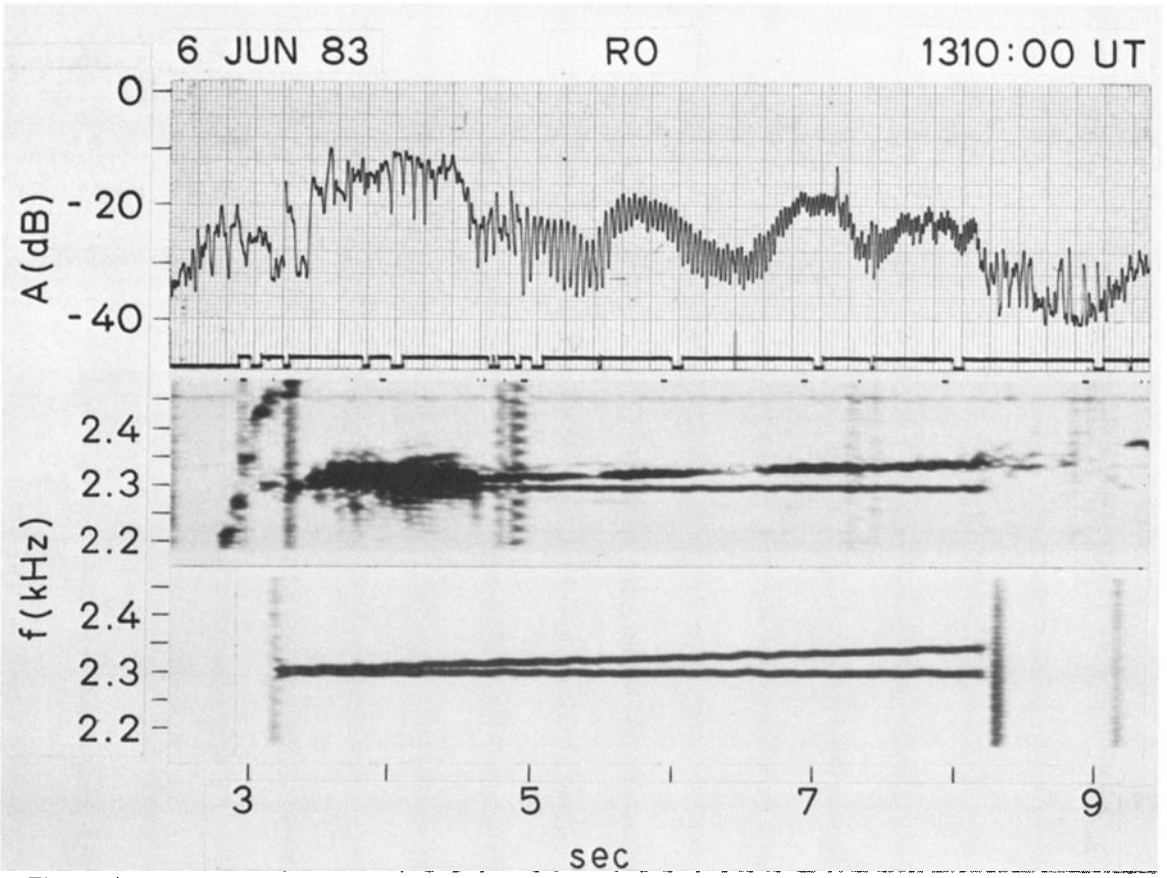

Fig. 5. A companion experiment to that illustrated in Figure 3. Here carriers f_1 and f_2 have equal intensities, but Δf increases linearly from 5 to 45 Hz over a 5-s interval.

filter bandwidths: 4 Hz, 20 Hz, and 80 Hz. The bottom panel shows amplitude in a 300-Hz band centered on the lower carrier f_1. Again in Figure 6*a*, as in Figure 3a, we see typical exponential growth when only a single frequency is present. When both transmitted signals are present (and equal in intensity), there is little or no growth of the individual components, as seen in the amplitude chart. The sideband structure is well defined with the 4-Hz bandwidth, but time resolution is poor. At 20 Hz we begin to see the fluctuations in the spectrum at the beat frequency, including variation in both frequency and amplitude. At 80 Hz we see more clearly the temporal behavior in amplitude and discover that each beat is accompanied by a second weaker signal that peaks approximately halfway between the beat peaks. This is a key finding. The same amplitude pattern is also seen in the wideband amplitude chart at the bottom of the record.

These effects are seen again in Figure 6*b*, recorded 24 seconds earlier with the tapered amplitude format of Figure 3*b* on the upper frequency. The emission between the beat peaks is stronger in this case, approaching or exceeding the intensity of a single carrier. The sideband structure for Figure 6*b* is shown in Figure 7. Here we see sidebands up to third order even when the two input signals are of equal intensity. As the intensity of the upper signal is reduced the sidebands become somewhat stronger, reaching about the same peak levels relative to the carriers as in the case of Figure 4.

The variable Δf format for this day is shown in Figure 8. Here the transition from moderate growth to suppression is not as sharp as in Figure 5. However, the sideband structure is broader than in Figure 5, as would be expected from Figures 6*a* and 6*b*. An interesting feature is the absence of the f_1 carrier at $\approx 1s$ in Figure 8. Multipath is an unlikely explanation since the dropout is so short (0.2 s). Such a dropout of one of the carriers is not uncommon and suggests that this carrier itself is being cancelled by a sideband at f_1 resulting from the presence of the upper carrier at f_2 and its sidebands. This result is understandable given the fact that the sideband and carriers have comparable amplitudes.

3. INTERPRETATION

The data presented in Figures 3, 5, 6, and 8 indicate that sidebands can be produced even when there is no temporal amplification of the injected signals. This finding is interesting since generation of coherent whistler mode signals has in the past been associated with nonlinear effects resulting from the trapping of the particles in the wave's potential well [*Dsythe*, 1971; *Bud'ko et al.*, 1972; *Serra*, 1984; *Bell*, 1985]. Satellite observations at $L = 4$ indicate that the intensity of unamplified signals from Siple Station is below the trapping threshold for cyclotron resonance, which is esimated to be ~1 pT for a pitch angle of 30° [*Helliwell and Inan*, 1982]. The measured intensities of Siple signals at high altitudes near the equatorial plane are typically 0.1–0.2 pT [*Inan et al.*, 1977; *Rastani et al.*, 1985]. Thus we are led to the conclusion that the trapping of resonant electrons in the potential well of the wave is not a necessary condition for generation of sidebands. Sideband generation

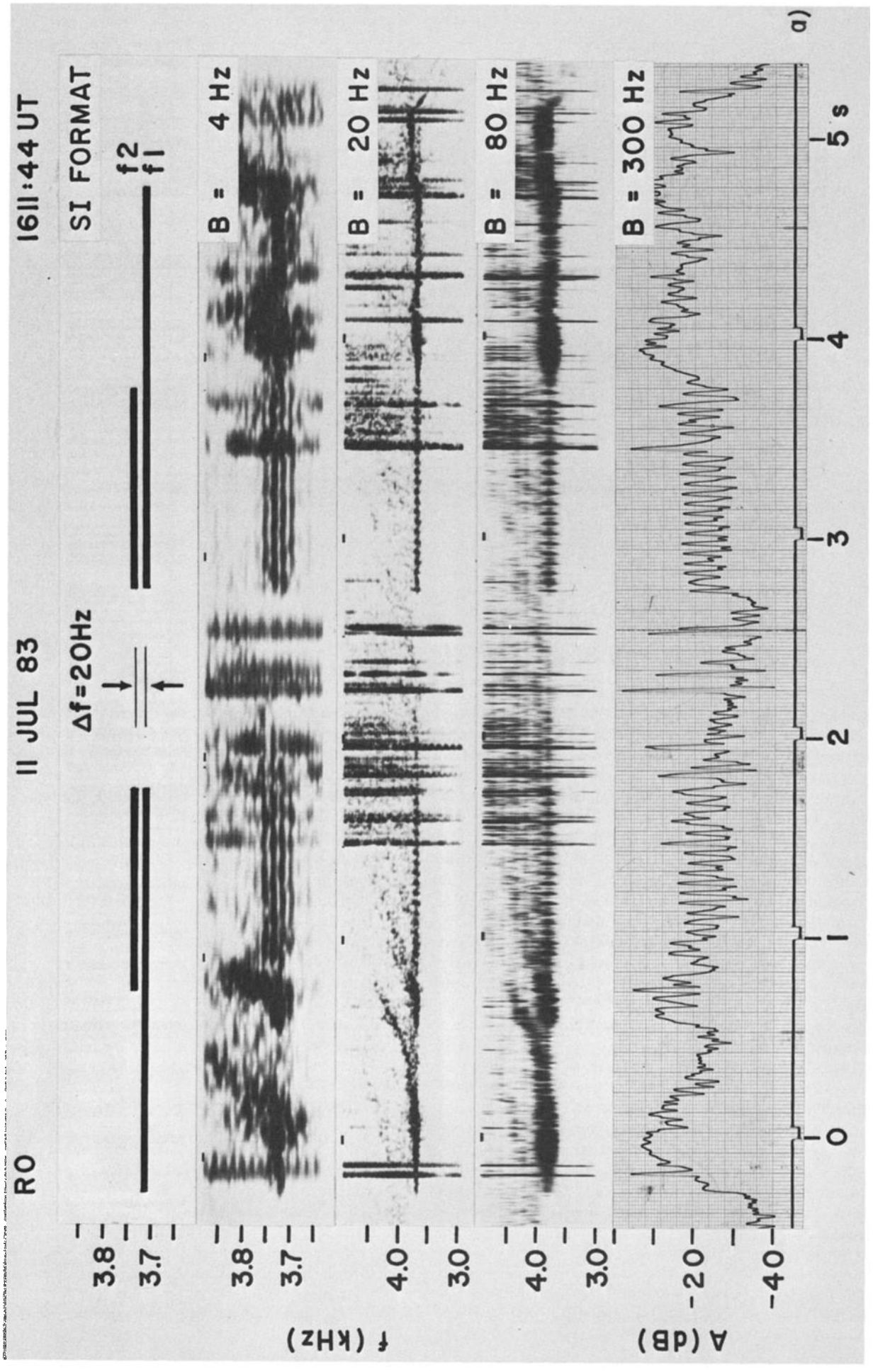
RO
11 JUL 83
1611:44 UT
SI FORMAT
Δf=20Hz
f2
f1
B = 4 Hz
B = 20 Hz
B = 80 Hz
B = 300 Hz
f (kHz)
A (dB)
3.8
3.7
4.0
3.0
-20
-40
0
1
2
3
4
5 s
a)

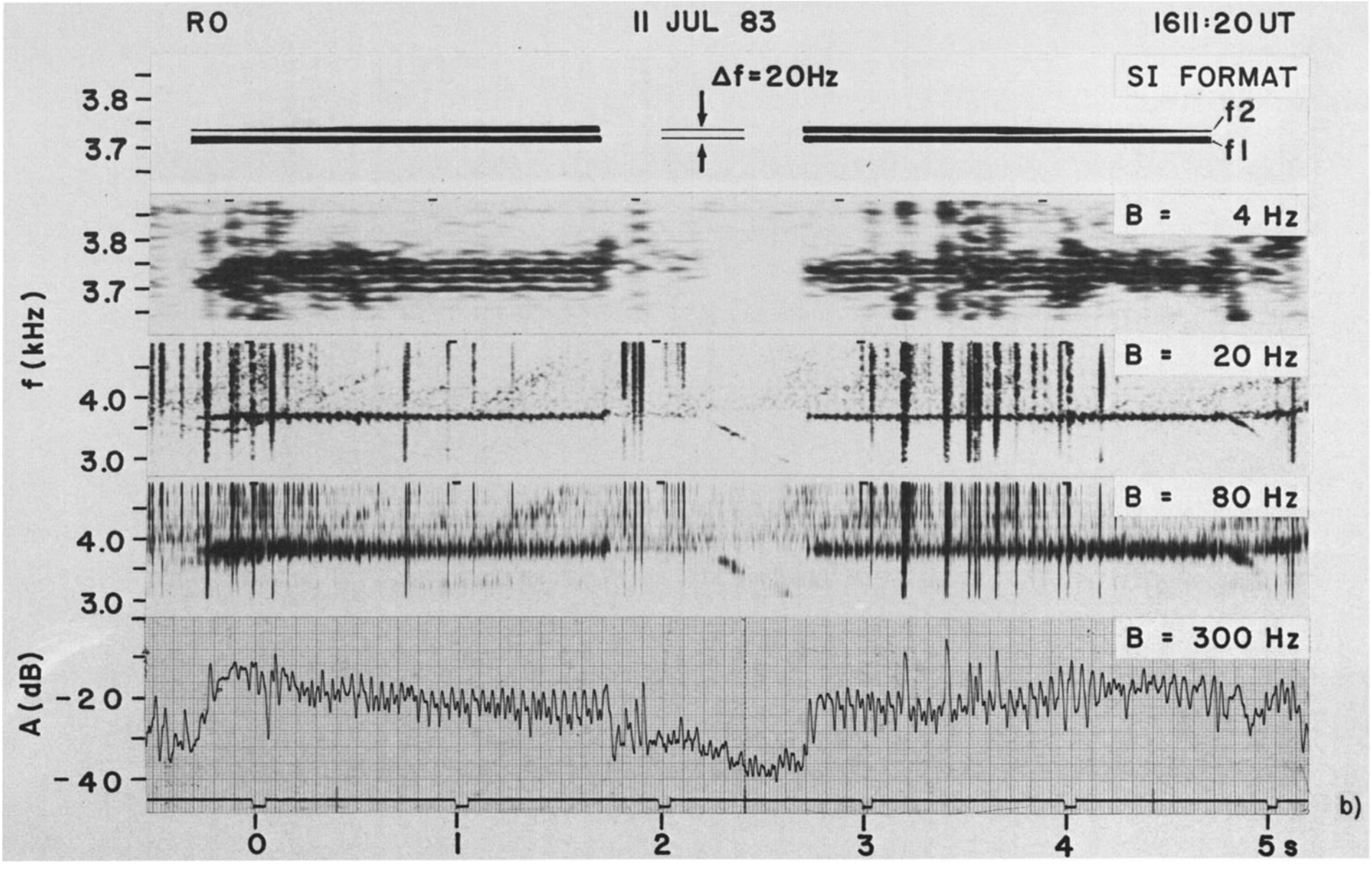

Fig. 6. Two-frequency response for July 11, 1983. The transmitted formats (top panels) are identical to those of Figure 3. Dynamic spectra are shown for three different analysis filter bandwidths: 4, 20, and 80 Hz. Broadband amplitude is shown in the lower panels and is obtained from a filter with a 300-Hz bandwidth, centered on the lower carrier. (*a*) From the lower panel, the single frequency exponential growth rate can be measured to be $\gamma \simeq 100$ dB/s, using the single-frequency pulse at the beginning of the record and again at 3.8 s when the upper signal is turned off.

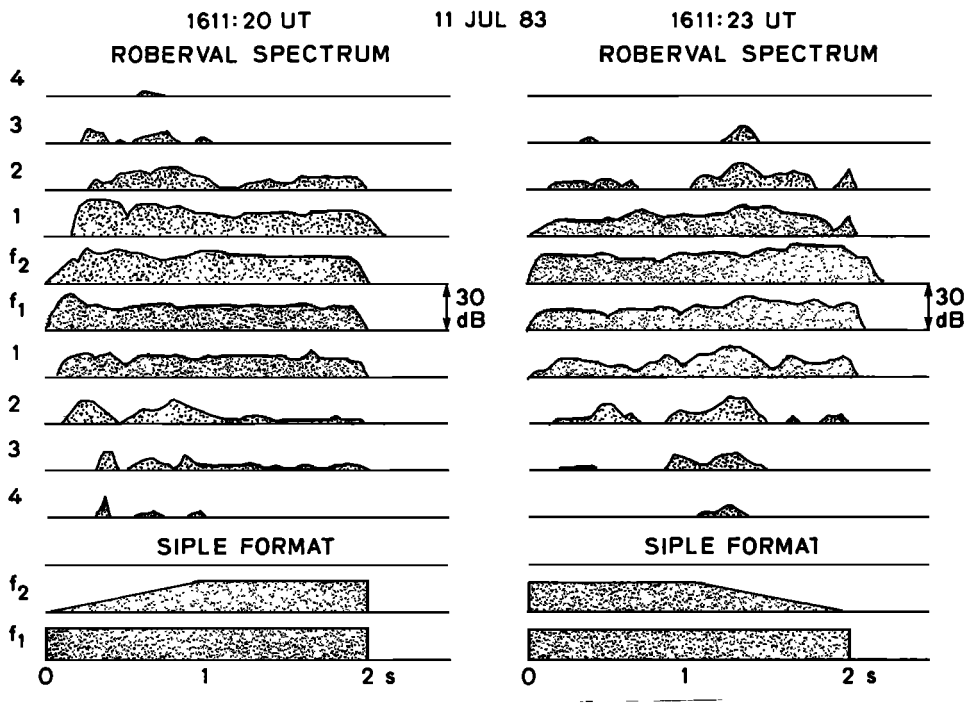

Fig. 7. Amplitude versus time for all components of the spectrum in Figure 6*b*.

based on quasi-linear diffusion at wave amplitudes below the trapping limit was proposed by *Ashour-Abdalla* [1972] and discussed by *Cornilleau-Wehrlin and Gendrin* [1979]. However this mechanism was shown to account for only small frequency separations (~10 Hz), whereas in the present experiment, sidebands are seen up to 100 Hz.

A possible explanation of the data in terms of the measured temporal growth rate in relation to the beat period is given below. The growth rate is ~100 dB/s as measured from the slopes of single frequency growth curves in Figures 3 and 5 whereas the beat period for 20 Hz separation is 50 ms. Assuming approximately exponential growth of a roughly equivalent (in terms of average) constant amplitude pulse of 30 ms duration, we would expect the total signal amplification to be 3 dB. While the applied input signal decreases to zero between the peaks of the beats, the emission that was generated by the preceding beat remains as the output signal.

A proposed mechanism for generation of sidebands is depicted in idealized form in Figure 9. Here each beat initiates an exponentially growing stimulated signal that is assumed to reach its maximum at the null of the beat. It then decays rapidly due to suppression by the following beat, giving rise to the waveform sketched in Figure 9. During the growth of the signal, the phase of the stimulated wave would be expected to advance, as has been shown to occur in stimulated emissions from the magnetosphere [*Paschal and Helliwell*, 1984]. The initial phase of the stimulated radiation with respect to the applied field is assumed to be $-\pi/2$ which corresponds to alignment of the phase bunched currents with the magnetic field of the applied beat wave. The postulated rate of phase advance as shown in Figure 9 is consistent with observed rates for triggered emissions [*Paschal and Helliwell*, 1984]. The corresponding instantaneous frequency, which is the time derivative of the phase, is shown by the dashed lines. The alternating phase of successive beats is represented in the diagram by shifting the phase reference by π radians every other beat. Thus the ϕ_s curves show an alternation in starting phase of π radians relative to the first beat whereas Δf is not affected by this initial condition.

By adding the stimulated emission B_s to the applied wave B_{in}, taking account of the instantaneous phase of B_s, the total output signal can be constructed in both amplitude and phase, assuming some phase shift due to dispersion. The result is shown in Figure 9*d*, where the magnitude of the total output signal is plotted as a function of time, together with the rate of change of the phase ($2\pi\Delta f$) of B_{out} with time. The predicted frequency changes (~50 Hz) are similar to those observed in Figure 6*b*. It should be noted that for the above first order calculation of B_{out} and Δf it is not possible to determine accurately the phasings of the different received components. One reason for this is the frequency changes (~50 Hz) shown in the middle panel. Whistler mode dispersion over the propagation path between the equatorial plane and the ground causes large phase shifts between the components. Accordingly phasings have been assumed such that $B_{out}(t)$ resembles the experimental data, for example in Figure 6*b*. The sketch of Figure 9 is intended only to establish the plausibility of the proposed mechanism for the creation of sidebands. In any case it is clear that the $B_{out}(t)$ curve cannot be decomposed into only two frequency components f_1 and f_2 but must contain sidebands. In general the frequencies of these sidebands will be $2f_2 - f_1$, $2f_1 - f_2$, etc.

4. SUMMARY AND DISCUSSION

In the light of the above results and discussion, it appears that sidebands can arise from a small signal triggering process in which the energy from the phase-bunched particles feeds preferentially into the sidebands rather than causing

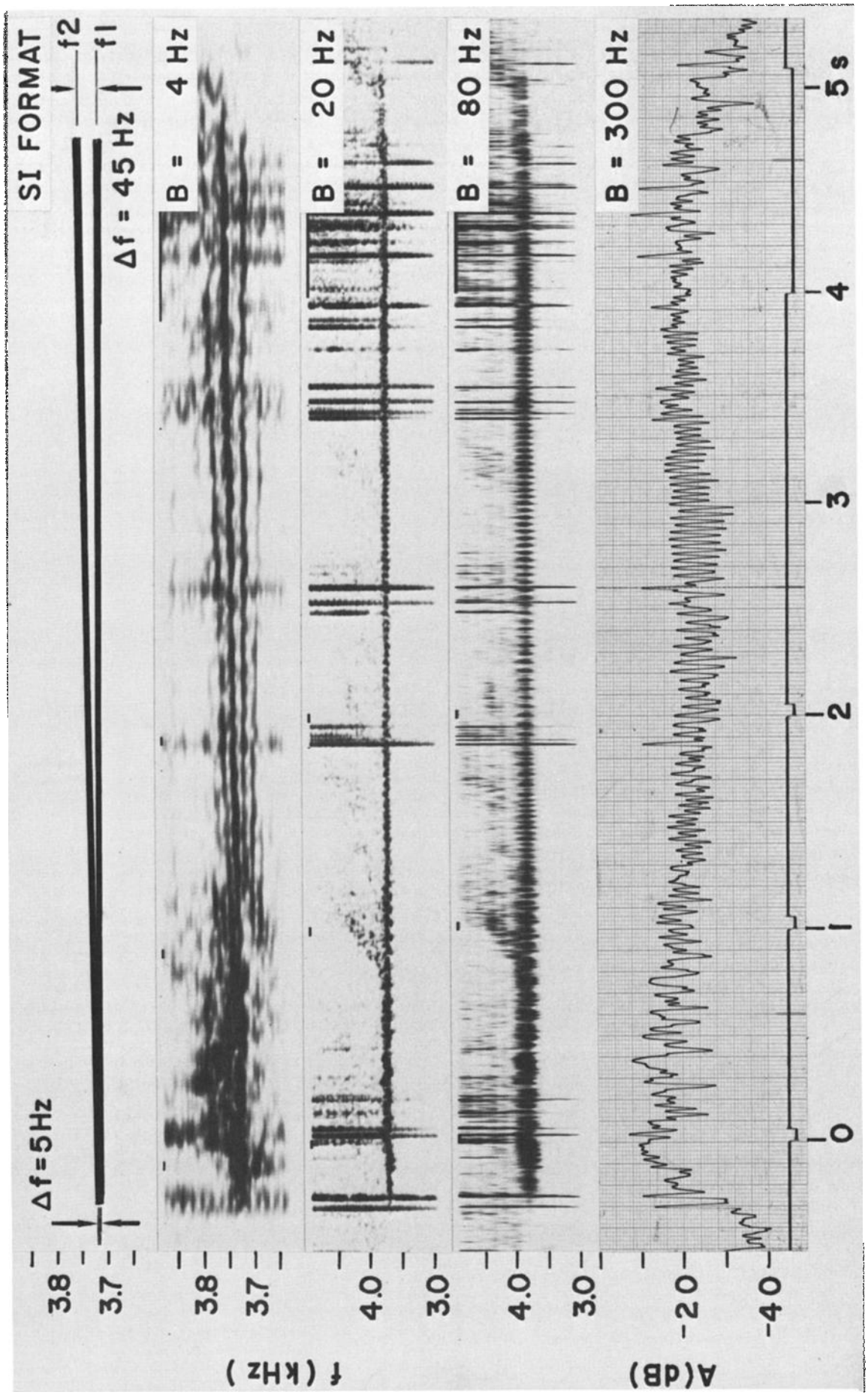

Fig. 8. A companion experiment to the ones illustrated in Figure 6. Transmitted format was similar to that of Figure 5.

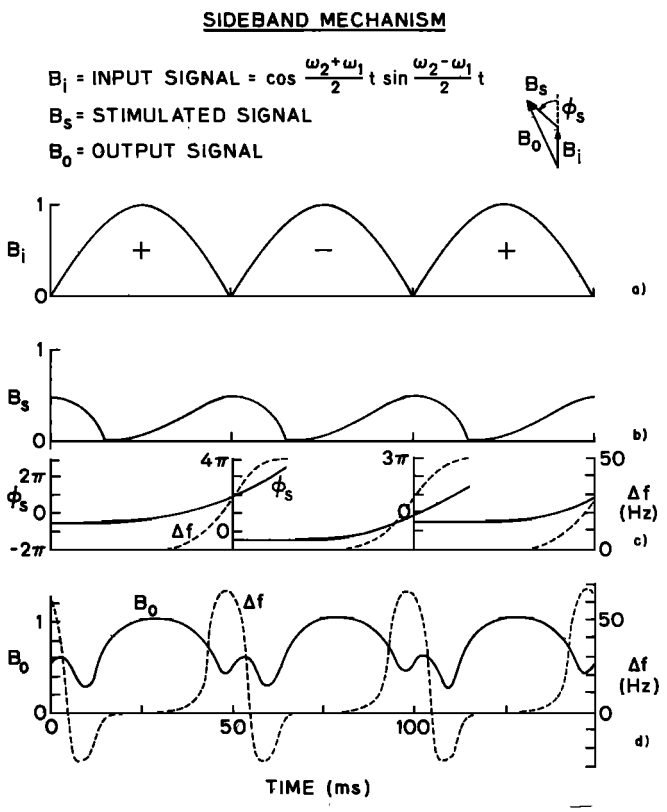

Fig. 9. Sideband generation mechanism. (*a*) Input beat signal, $\Delta f = 20$ Hz. (*b*) Postulated signal (*BS*) triggered by beat, assuming 80 dB/s average growth rate during beat. (*c*) Frequency change Δf (dashed curves) estimated from Figure 6*b*, and associated phase ϕ_s, derived from $\Delta f(t)$. (*d*) A possible output signal intensity and Δf calculated that is consistent with Figures 9*a*–9*c*.

growth of the input waves themselves. Thus the presence of two signals propagating in the magnetosphere and having frequency spacing ~10–100 Hz can lead to significant sidebands which may extend as much as ±100 Hz with respect to the average frequency of the pair. Thus new frequencies of significant magnitude can be created with little or no growth of the input signals. On the other hand, if the ratio of the two signals departs from unity, the stronger (~12–15 dB) signal will grow significantly, and even larger sidebands may be created. The energy in the sidebands in such a case can equal or exceed the energy in the injected carriers, as shown in Figure 7.

The process of sideband generation as reported in this paper will tend to break down the coherence of relatively narrowband injected waves. Thus power line harmonics, VLF transmitter signals, and whistlers interacting with one another in the magnetosphere would tend to be transformed from relatively coherent wave packets into broader, more variable bands of noiselike signals. Spectrum spreading, through the sideband generation process just described, combined with whistler mode echoing [*Helliwell*, 1965] would have the effect of filling up the available space in the frequency-time plane, with the separations between the sideband components tending to lie in the ~10–100 Hz range. The triggering of variable frequency emissions will tend further to alter the frequency relationships of these components, leading to a noiselike spectrum similar to that of mid-latitude hiss.

Phase trapping of resonant electrons by the wave is not required for the generation of sidebands in our proposed model, either with or without temporal growth of the input signals. While this conclusion does not necessarily contradict other suggested sideband theories that depend on trapping [*Brinca*, 1972; *Nunn*, 1974; *Serra*, 1984], the beat-triggering mechanism suggested here could potentially account for some or all of the observed cases of sideband generation, including those recently reported on nonducted signals [*Bell*, 1985]. The key factor in resolving this question is the input signal strength in the postulated interaction region (see Figure 1). Although satellite data give consistent values (~0.01–0.2 pT) of nonducted Siple signals [*Inan et al.*, 1977; *Rastani et al.*, 1985], we cannot conclude that ducted signals would necessarily have the same intensity just before temporal growth occurs. It is possible that significant spatial growth occurs preferentially within a duct, causing the input to the temporal growth region to exceed the trapping threshold of about 1 pT [*Dowden et al.*, 1978]. On the other hand, even if such were the case, the sideband mechanism we have outlined would still be plausible.

Finally, we note that the mechanism described in the previous section is based only on observed wave growth rates and the accompanying phase advance. It is thus independent of the exact mechanism of generation. The details of the growth and emission triggering processes and their relation to the energetic particle distribution function remain to be determined [*Helliwell and Inan*, 1982].

Acknowledgments. We thank T. F. Bell for helpful comments on the manuscript. We also thank D. Shafer for his efforts as a winter-over scientist at Siple Station. The spectrograms in this paper were prepared by J. Yarbrough, while the spectral amplitudes of Figures 4 and 6 were scaled and plotted by Philip Lorch. The manuscript was prepared by G. Walker. This work is supported by the Division of Polar Programs of the National Science Foundation under grants DPP-83-17092 and DPP-83-18508.

The Editor thanks N. Cornilleau-Wehrlin and T. J. Rosenberg for their assistance in evaluating this paper.

REFERENCES

Ashour-Abdalla, M., Amplification of whistler waves in the magnetosphere, *Planet. Space Sci., 20,* 639, 1972.

Bell, T. F., High-amplitude VLF transmitter signals and associated sidebands observed near the magnetic equatorial plane on the ISEE-1 satellite, *J. Geophys. Res., 90,* 1771, 1985.

Brinca, A. L., Whistler sideband growth due to nonlinear wave particle interaction, *J. Geophys. Res., 77,* 3508, 1972.

Bud'ko, N. I., V. I. Karpman, and O. A. Pokshtelov, Nonlinear theory of the monochromatic circularly polarized VLF and ULF waves in the magnetosphere, *Cosmic Electrodyn., 3,* 147, 1972.

Carlson, C. R., R. A. Helliwell, and D. L. Carpenter, Variable frequency VLF signals in the magnetosphere: associated phenomena and plasma diagnostics, *J. Geophys. Res., 90,* 1507, 1985.

Cornilleau-Wehrlin, N., and R. Gendrin, VLF transmitter-induced quiet bands: A quantitative interpretation, *J. Geophys. Res., 84,* 882, 1979.

Dowden, R. L., A. C. McKey, L. E. S. Amon, H. C. Koons, and M. H. Dazey, Linear and nonlinear amplification in the magnetosphere during a 6.6 kHz transmission, *J. Geophys. Res., 83,* 169, 1978.

Dsythe, K. B., Some studies of triggered whistler emissions, *J. Geophys. Res., 76,* 6915, 1971.

Helliwell, R. A., *Whistlers and Related Ionospheric Phenomena,* Stanford University Press, Stanford, Calif., 1965.

Helliwell, R. A., Controlled stimulation of VLF emissions from Siple Station, Antarctica, *Radio Sci., 6,* 801, 1983.

Helliwell, R. A., and U. S. Inan, VLF wave growth and discrete emission triggering in the magnetosphere: A feedback model, *J. Geophys. Res., 87*, 3537, 1982.

Helliwell, R. A. and J. P. Katsufrakis, VLF wave injection experiments into the magnetosphere from Siple Station, Antarctica, *J. Geophys. Res., 79*, 2511, 1974.

Helliwell, R. A., and J. P. Katsufrakis, Controlled wave-particle interaction experiments, in *Upper Atmosphere Research in Antarctica, Antarctic Res. Ser. vol. 29*, edited by L. J. Lanzerotti and C. G. Park, p. 100, AGU, Washington, D. C., 1978.

Helliwell, R. A., S. B. Mende, J. H. Doolittle, W. C. Armstrong, and D. L. Carpenter, Correlations between λ4278 optical emissions and VLF wave events observed at $L \sim 4$ in the Antarctic, *J. Geophys. Res., 85*, 3376, 1980.

Inan, U. S., T. F. Bell, D. L. Carpenter, and R. R. Anderson, Explorer 45 and Imp 6 observations in the magnetosphere of injected waves from the Siple Station VLF transmitter, *J. Geophys. Res., 82*, 1177, 1977.

Inan, U. S., T. F. Bell, and H. C. Chang, Particle precipitation induced by short-duration VLF waves in the magnetosphere, *J. Geophys. Res., 87*, 6243, 1982.

Matsumoto, H., Nonlinear whistler mode interaction and triggered emissions in the magnetosphere: a review, in *Wave Instabilities in Space Plasmas*, edited by P. J. Palmadesso and K. Papadopoulos, p. 163, D. Reidel, Hingham, Mass., 1979.

Nunn, D., A self-consistent theory of triggered VLF emissions, *Planet. Space Sci., 22*, 349, 1974.

Park, C. G., and D. L. Carpenter, Very low frequency radio waves in the magnetosphere, in *Upper Atmosphere Research in Antarctica, Antarctic Res. Ser. vol. 29*, edited by L. J. Lanzerotti and C. G. Park, p. 72, AGU, Washington, D. C., 1978.

Paschal, E. W. and R. A. Helliwell, Phase measurements of whistler mode signals from the Siple VLF transmitter, *J. Geophys. Res., 89*, 1667, 1984.

Raghuram, R., T. F. Bell, R. A. Helliwell, and J. P. Katsufrakis, Quiet band produced by VLF transmitter signals in the magnetosphere, *Geophys. Res. Lett., 4*, 199, 1977.

Rastani, K., U. S. Inan, and R. A. Helliwell, DE 1 observations of Siple transmitter signals and associated sidebands, *J. Geophys. Res., 90*, 4128, 1985.

Rosenberg, T. J., R. A. Helliwell, and J. P. Katsufrakis, Electron precipitation associated with discrete very-low-frequency emissions, *J. Geophys. Res., 76*, 8445, 1971.

Serra, F. M., On the suppression of wave growth and triggering in VLF multi-wave experiments, *Planet. Space Sci., 32*, 1577, 1984.

D. L. Carpenter, R. A. Helliwell, U. S. Inan, and J. P. Katsufrakis, Space, Telecommunications, and Radioscience Laboratory, Stanford University, Stanford, CA 94305.

(Received July 11, 1985;
revised September 9, 1985;
accepted September 10, 1985.)